Journal of
Mechanics of
Materials and Structures

DYNAMIC RESPONSE OF MULTIPLE FLEXIBLE STRIPS ON A MULTILAYERED POROELASTIC HALF-PLANE

Teerapong Senjuntichai and Wichairat Kaewjuea

Volume 3, Nº 10 December 2008

mathematical sciences publishers

JOURNAL OF MECHANICS OF MATERIALS AND STRUCTURES
Vol. 3, No. 10, 2008

DYNAMIC RESPONSE OF MULTIPLE FLEXIBLE STRIPS ON A MULTILAYERED POROELASTIC HALF-PLANE

TEERAPONG SENJUNTICHAI AND WICHAIRAT KAEWJUEA

We study the dynamic response of multiple flexible strip foundations resting on a multilayered poroelastic half-plane subjected to time-harmonic vertical loading. The contact surface between the strip foundations and the half-plane is assumed to be smooth and either fully permeable or impermeable. The half-plane under consideration consists of a number of layers with different thicknesses and material properties, and is governed by Biot's poroelastodynamic theory. The vertical deflection of the strip foundation is represented by an admissible function containing a set of generalized coordinates. Solutions for generalized coordinates are obtained by establishing the equations of motion of the foundation through the application of Lagrange's equations of motion. Selected numerical results are presented to demonstrate the influence of foundation rigidity, hydraulic boundary conditions, layer properties and configuration, and distance of adjacent foundations on dynamic interaction between flexible strip foundations and a multilayered poroelastic half-plane.

1. Introduction

The study of dynamic interaction between a strip foundation and an elastic medium has received considerable attention over the past forty years due to its useful applications for analysis and design of foundations subjected to dynamic loading. Mixed-boundary value problems related to vibrations of a strip foundation have been considered in the past by employing a variety of analytical, semianalytical, and numerical techniques. Karasudhi et al. [1968] derived analytical solutions for vertical, horizontal, and rocking vibrations of a rigid smooth strip resting on an elastic half-plane in terms of Fredholm integral equations. The integral equation solutions were also presented by Luco and Westmann [1972] for dynamic response of a surface rigid strip bonded to an elastic half-plane. Gazetas and Roesset [1976] employed a semianalytical technique to obtain dynamic compliances of a rigid strip on a layered elastic medium. Dynamic interaction between a system of flexible strips and an elastic half-plane was studied by Wang et al. [1991] by employing a coupled variational-Green's function technique. Several researchers have employed numerical approaches to study vibrations of a strip foundation. For example, Chang-Liang [1974] presented a finite element model of a strip footing on an elastic layer with rigid base. A boundary element method was used by Israil and Ahmad [1989] to study dynamic interaction between a rigid strip and a layered viscoelastic medium. In addition, a number of studies related to vibrations of flexible strips have been presented [Spyrakos and Beskos 1986; Kokkinos and Spyrakos 1991; Spyrakos and Xu 2004] by employing a hybrid BEM-FEM technique.

Keywords: multiple strip foundations, layered systems, poroelasticity, soil-structure interaction, vibrations.
The work presented in this paper was partially supported by CHE and AUN/SEED-Net Scholarships. This support is gratefully acknowledged.

All studies mentioned above considered a half-plane as a single-phase elastic medium. However, geomaterials are often two-phased materials with a solid skeleton and pores filled with water, commonly known as poroelastic materials in mechanics literature. The first theory of elastic wave propagation in a poroelastic medium was established by Biot [1956] by adding inertia terms to his quasistatic theory [Biot 1941]. A limited number of studies related to vibrations of a rigid strip foundation on a poroelastic medium have appeared in the literature by employing Biot's poroelastodynamic theory despite their relavance to geotechnical engineering and earthquake engineering [Kassir and Xu 1988; Bougacha et al. 1993; Japón et al. 1997]. In addition, dynamic response of a rigid strip bonded to a multilayered poroelastic half-plane was also studied by Senjuntichai and Rajapakse [1996] by employing an exact stiffness matrix scheme [Rajapakse and Senjuntichai 1995] and a discretization technique. In practice, there exists a situation of a closely spaced foundation system where one needs to consider not only the interaction between the foundations and the supporting medium but also the interaction that occurs between the adjacent foundations through the supporting medium. A review of literature indicates that this structure-soil-structure interaction problem has been investigated in the past for dynamic interaction between elatic media and rigid circular foudations [Warburton et al. 1971; Wong and Luco 1986], and flexible strip foundations [Wang et al. 1991]. To our knowledge, the dynamic interaction between a system of foundations and a poroelastic medium has never been reported in the literature.

In this paper, the dynamic response of a system of flexible strip foundations resting on a multilayered poroelastic half-plane subjected to time-harmonic vertical loading as shown in Figure 1 is studied. The interaction problem is analyzed by adopting the coupled variational Green's function scheme [Wang et al. 1991] together with a discretization technique. The contact surface between the foundations and the half-plane is assumed to be smooth. Two extreme fluid flow conditions at the strip-half-plane contact surface are considered, that is, fully permeable and impermeable contact surfaces. Each layer of the half-plane is governed by Biot's theory of poroelastodynamics. The transverse deflection of a strip foundation is represented by an admissible function containing a set of generalized coordinates. Contact traction and pore pressure jump under each strip foundation are expressed in term of the generalized coordinates through the solutions of the flexibility equations based on the influence functions. These influence functions correspond to the solid and fluid displacements of a multilayered half-plane under a vertical load and pore pressure loading at the surface level. The generalized coordinates are determined by establishing the Lagrange equations of motion for the foundation system. Convergence and accuracy of the present numerical scheme are established through comparison with existing studies. Selected numerical results are presented to illustrate the influence of poroelastic material parameters, layering, foundation rigidity, hydraulic boundary conditions, frequency of excitation, and presence of adjacent foundations on vertical displacement, contact traction, and pore pressure profiles, and bending moment of the strip foundation system.

2. Basic equations and influence functions

Consider a poroelastic medium with a Cartesian coordinate system (x, y, z) defined such that the z-axis is perpendicular to the free surface as shown in Figure 1. It is assumed that the deformations are plane strain in the xz-plane, that is, $\varepsilon_{xy} = \varepsilon_{yy} = \varepsilon_{yz} = 0$. Let u_i and w_i denote the average displacement of the solid matrix and the fluid displacement relative to the solid matrix in the i-direction $(i = x, z)$ respectively.

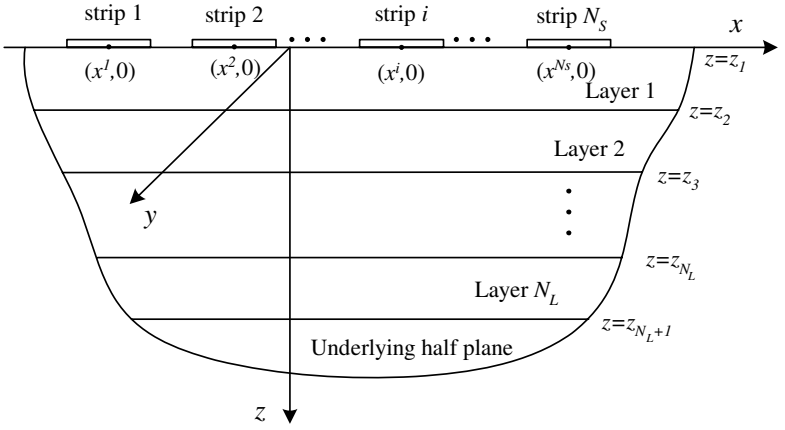

Figure 1. Flexible strip foundations on a multilayered poroelastic half-plane.

The constitutive relations for a homogeneous poroelastic material [Biot 1941] can be expressed by using standard indicial notations as $\sigma_{ij} = 2\mu\varepsilon_{ij} + \lambda\delta_{ij}\varepsilon_{kk} - \alpha\delta_{ij}p$, with $i, j = x, z$, and $p = -\alpha M\varepsilon_{kk} + M\zeta$. In the above equations, σ_{ij} and ε_{ij} denote the stresses and strains of the bulk material respectively, μ and λ are Lame's constants of the bulk material, p is the excess pore fluid pressure (suction is considered negative), ζ is the variation of the fluid content per unit reference volume defined as $\zeta = -w_{i,i}$, and δ_{ij} denotes the Kronecker delta. In addition, α and M are Biot's parameters accounting for the compressibility of the two-phase material.

The equations of motion for a poroelastic medium in the absence of body forces (solid and fluid) and a fluid source can be expressed in terms of displacements u_i and w_i as [Biot 1962]

$$\begin{aligned} \mu u_{i,jj} + (\lambda + \alpha^2 M + \mu) u_{j,ji} - \alpha M w_{j,ji} &= \rho\ddot{u}_i + \rho_f \ddot{w}_i, \\ \alpha M u_{j,ji} + M w_{j,ji} &= \rho_f \ddot{u}_i + m\ddot{w}_i + b\dot{w}_i. \end{aligned} \tag{1}$$

Here ρ and ρ_f are the mass densities of the bulk material and the pore fluid respectively, m is a density parameter that depends on ρ_f and the geometry of the pores, and b is the parameter accounting for the internal friction due to the relative motion between the solid matrix and the pore fluid. If the internal friction is neglected, then $b = 0$. In addition, the superscript dot denotes the derivative with respect to time.

The motion under consideration is time-harmonic with a factor $e^{i\omega t}$ where ω is the frequency of motion and $i = \sqrt{-1}$. The term $e^{i\omega t}$ is hereafter omitted from all expressions for brevity.

The Fourier integral transform of a function $f(x, z)$ and its inverse relationship with respect to the x-coordinate are given by [Sneddon 1951]

$$\bar{f}(\xi, z) = \frac{1}{\sqrt{2\pi}} \int_{-\infty}^{\infty} f(x, z) e^{-i\xi x}\, dx, \qquad f(x, z) = \frac{1}{\sqrt{2\pi}} \int_{-\infty}^{\infty} \bar{f}(\xi, z) e^{i\xi x}\, d\xi, \tag{2}$$

where ξ denotes the Fourier transform parameter.

An exact stiffness matrix method proposed by Rajapakse and Senjuntichai [1995] is employed in the derivation of the influence functions required for analysis of the interaction problem shown in Figure 1.

In this method, the exact stiffness matrices for the nth layer and an underlying half-plane are derived from the general solutions of a homogeneous poroelastic material in the Fourier transform space [Senjuntichai and Rajapakse 1994]. The global stiffness matrix of a multilayered poroelastic half-plane is then obtained by assembling the layer and half-plane stiffness matrices together with the continuity of traction and fluid flow at the layer interfaces. The global equation system can be expressed as

$$\boldsymbol{K}\boldsymbol{U} = \boldsymbol{F}, \tag{3}$$

where $\boldsymbol{K}$ is the global stiffness matrix, $\boldsymbol{U}$ and $\boldsymbol{F}$ are the global vectors of generalized displacements and generalized forces defined as

$$\boldsymbol{U} = \left[u^{(2)} \;\; u^{(2)} \;\; \cdots \;\; u^{(n)} \;\; \cdots \;\; u^{(N)} \;\; u^{(N+1)}\right]^T, \qquad \boldsymbol{F} = \left[f^{(1)} \;\; f^{(2)} \;\; \cdots \;\; f^{(n)} \;\; \cdots \;\; f^{(N)} \;\; f^{(N+1)}\right]^T,$$

in which

$$\boldsymbol{u}^{(n)} = \left[i\bar{u}_x^{(n)} \;\; \bar{u}_z^{(n)} \;\; \bar{p}^{(n)}\right]^T, \qquad \boldsymbol{f}^{(n)} = \left[i\bar{\sigma}_{zx}^{(n)} \;\; \bar{\sigma}_{zz}^{(n)} \;\; \bar{w}_z^{(n)}\right]^T,$$

and the superscript n denotes the quantities at the nth interface. Details on the formulation of the exact stiffness matrix method including the explicit expression of the layer and half-plane stiffness matrices are given elsewhere [Rajapakse and Senjuntichai 1995].

To determine the influence functions, a boundary value problem corresponding to a multilayered poroelastic half-plane subjected to a uniform strip load at the surface is solved. The global generalized force vector can then be expressed as

$$\boldsymbol{F} = \left[0 \;\; -\sqrt{\frac{2}{\pi}}\frac{\sin(\xi a)}{\xi} \;\; 0 \;\cdots\; 0\right]^T,$$

where a is half the width of the loading strip. The solutions for displacements and pore pressure at layer interfaces can be obtained by solving (3) for discrete value of ξ together with the application of numerical quadrature to evaluate the inverse Fourier transforms defined in (2). In the analysis of the interaction problem shown in Figure 1, only vertical solid and fluid displacements (u_z and w_z) at the surface level are required to establish the flexibility equation for the derivation of the contact stress and pore pressure jump, which are employed in the formulation presented in the next section.

3. Formulation of interaction problem

Consider a system of N_S flexible foundations resting on a multilayered poroelastic medium as shown in Figure 1. For a foundation with its length much longer than its width subjected to dynamic loading that is uniform along the longitudinal direction, it is reasonable to consider the foundation as a strip foundation under plane strain condition. For the i-th strip foundation with a width of $2a^i$, it is convenient to define a local coordinate η as $\eta = (x - x^i)/a^i$, with $i = 1, 2, 3, \ldots, N_S$, where x^i is the x-coordinate at the center of the i-th foundation. The vertical deflection of the i-th foundation, denoted by w_{st}^i, can then be expressed as

$$w_{st}^i(\eta) = \sum_{n=0}^{N_T} \alpha_n^i \eta^n, \qquad i = 1, 2, 3, \ldots, N_S, \tag{4}$$

where $\alpha_0^i, \alpha_1^i, \ldots, \alpha_{N_T}^i$ are a set of generalized coordinates. In view of (4), the bending moment per unit length acting on the i-th foundation is given by

$$M_{st}^i(\eta) = -D^i \sum_{n=0}^{N_T} n(n-1)\alpha_n^i \eta^{n-2}, \quad i = 1, 2, 3, \ldots, N_S, \qquad \text{where} \qquad D^i = \frac{E_{st}^i (h_{st}^i)^3}{12\left[1-(\nu_{st}^i)^2\right]},$$

and h_{st}^i, E_{st}^i, and ν_{st}^i are the thickness, Young's modulus, and Poisson's ratio of the i-th foundation.

In this paper, it is assumed that the contact surface between the strip foundation and the multilayered half-plane is smooth and either fully permeable or impermeable. For an impermeable strip foundation, the vertical loading is resisted by contact traction and pore pressure generated at the bottom surface of the foundation. The resultants of the contact traction and pore pressure of the i-th foundation can be represented by traction $T_z^i(\eta)$ and pore pressure jump $T_p^i(\eta)$ acting on the contact surface between the i-th foundation and the half-plane.

To determine T_z^i and T_p^i, the contact surface between the i-th strip foundation ($i = 1, 2, 3, \ldots, N_S$) and the half-plane is discretized into the total number of N_E^i strip elements. The width of each element is denoted by Δ_k^i where $k = 1, 2, \ldots, N_E^i$ (see Figure 2). The vertical displacement compatibility and the impermeable condition are then imposed at the contact surface between the strip foundation and the half-plane. This is done by taking each term of the deflection approximation of the i-th foundation, (4) with $\alpha_n^i = 1$ ($i = 1, 2, 3, \ldots, N_S$; $n = 0, 1, 2, \ldots, N_T$). Thereafter, the resulting deflection variation and zero flow condition are imposed on the nodal locations at the contact surface of the half-plane by applying contact traction T_{znk}^i and pore pressure jump T_{pnk}^i at the k-th node of the i-th strip foundation. It is assumed that contact traction and pore pressure jump are constant within each strip element. The following flexibility equation system can be established to determine the intensities of T_{znk}^i and T_{pnk}^i at each strip element:

$$\begin{bmatrix} \boldsymbol{G}_{zz}^{11} & \boldsymbol{G}_{zp}^{11} & \cdots & \boldsymbol{G}_{zr}^{1j} & \cdots & \boldsymbol{G}_{zz}^{1N_S} & \boldsymbol{G}_{zp}^{1N_S} \\ \boldsymbol{G}_{pz}^{11} & \boldsymbol{G}_{pp}^{11} & \cdots & \boldsymbol{G}_{pr}^{1j} & \cdots & \boldsymbol{G}_{pz}^{1N_S} & \boldsymbol{G}_{pp}^{1N_S} \\ \vdots & \vdots & \ddots & \vdots & \iddots & \vdots & \vdots \\ \boldsymbol{G}_{qz}^{i1} & \boldsymbol{G}_{qp}^{i1} & \cdots & \boldsymbol{G}_{qr}^{ij} & \cdots & \boldsymbol{G}_{qz}^{iN_S} & \boldsymbol{G}_{qp}^{iN_S} \\ \vdots & \vdots & \iddots & \vdots & \ddots & \vdots & \vdots \\ \boldsymbol{G}_{zz}^{N_S1} & \boldsymbol{G}_{zp}^{N_S1} & \cdots & \boldsymbol{G}_{zr}^{N_Sj} & \cdots & \boldsymbol{G}_{zz}^{N_SN_S} & \boldsymbol{G}_{zp}^{N_SN_S} \\ \boldsymbol{G}_{pz}^{N_S1} & \boldsymbol{G}_{pp}^{N_S1} & \cdots & \boldsymbol{G}_{pr}^{N_Sj} & \cdots & \boldsymbol{G}_{pz}^{N_SN_S} & \boldsymbol{G}_{pp}^{N_SN_S} \end{bmatrix} \begin{Bmatrix} \boldsymbol{T}_{zn}^1 \\ \boldsymbol{T}_{pn}^1 \\ \vdots \\ \boldsymbol{T}_{qn}^i \\ \vdots \\ \boldsymbol{T}_{zn}^{N_S} \\ \boldsymbol{T}_{pn}^{N_S} \end{Bmatrix} = \begin{Bmatrix} \boldsymbol{u}_{zn}^1 \\ \boldsymbol{u}_{pn}^1 \\ \vdots \\ \boldsymbol{u}_{qn}^i \\ \vdots \\ \boldsymbol{u}_{zn}^{N_S} \\ \boldsymbol{u}_{pn}^{N_S} \end{Bmatrix}, \tag{5}$$

where

$$\boldsymbol{G}_{qr}^{ij} = \begin{bmatrix} G_{qr,11}^{ij} & G_{qr,12}^{ij} & \cdots & G_{qr,1N_E}^{ij} \\ G_{qr,21}^{ij} & G_{qr,22}^{ij} & \cdots & G_{qr,2N_E}^{ij} \\ \vdots & \vdots & G_{qr,kl}^{ij} & \vdots \\ G_{qr,N_E1}^{ij} & G_{qr,N_E2}^{ij} & \cdots & G_{qr,N_EN_E}^{ij} \end{bmatrix}.$$

In this equation, the element $G_{qr,kl}^{ij}$ ($i, j = 1, 2, 3, \ldots, N_S$; $k, l = 1, 2, 3, \ldots, N_E$) denotes the vertical displacement ($q = z$) and the fluid displacement ($q = p$) at the center of the k-th strip element of the i-th foundation due to a vertical load ($r = z$) and fluid pressure ($r = p$) applied over the l-th strip element of

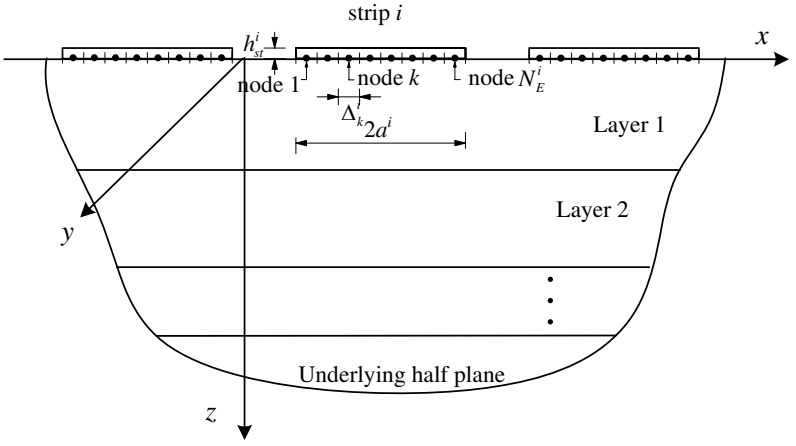

Figure 2. Dicretization of the strip-half-plane contact surface.

the j-th foundation. In addition,

$$\boldsymbol{T}^i_{zn} = \begin{bmatrix} T^i_{zn1} & T^i_{zn2} & \cdots & T^i_{znk} & \cdots & T^i_{znN_E} \end{bmatrix}^T, \qquad \boldsymbol{T}^i_{pn} = \begin{bmatrix} T^i_{pn1} & T^i_{pn2} & \cdots & T^i_{pnk} & \cdots & T^i_{pnN_E} \end{bmatrix}^T,$$
$$\boldsymbol{u}^i_{zn} = \begin{bmatrix} u^i_{zn1} & u^i_{zn2} & \cdots & u^i_{znk} & \cdots & u^i_{znN_E} \end{bmatrix}^T, \qquad \boldsymbol{u}^i_{pn} = \begin{bmatrix} 0 & 0 & \cdots & 0 & \cdots & 0 \end{bmatrix}^T.$$

The contact traction and pore pressure jump at the k-th strip element of the i-th foundation that are required to satisfy the displacement compatibility and the impermeability condition at the contact surface can be expressed respectively as

$$T^i_{zk} = \sum_{n=0}^{N_T} \alpha^i_n T^i_{znk}, \qquad T^i_{pk} = \sum_{n=0}^{N_T} \alpha^i_n T^i_{pnk}, \tag{6}$$

where T^i_{znk} and T^i_{pnk} $(n = 0, 1, 2, \ldots, N_T; k = 1, 2, 3, \ldots, N_E)$ denote the intensities of contact traction and pore pressure jump respectively acting on the k-th strip element of the i-th foundation when $u^i_{znk} = \eta^n_k$, in which η_k is the local coordinate at the center of the k-th strip element.

For a fully permeable strip foundation, since no pore pressure jump is generated under the foundation, the flexibility matrix (5) is then reduced to

$$\begin{bmatrix} \boldsymbol{G}^{11}_{zz} & \boldsymbol{G}^{12}_{zz} & \cdots & \boldsymbol{G}^{1N_S}_{zz} \\ \boldsymbol{G}^{12}_{zz} & \boldsymbol{G}^{22}_{zz} & \cdots & \boldsymbol{G}^{2N_S}_{zz} \\ \vdots & \vdots & \boldsymbol{G}^{ij}_{zz} & \vdots \\ \boldsymbol{G}^{N_S1}_{zz} & \boldsymbol{G}^{N_S2}_{zz} & \cdots & \boldsymbol{G}^{N_SN_S}_{zz} \end{bmatrix} \begin{Bmatrix} \boldsymbol{T}^1_{zn} \\ \boldsymbol{T}^2_{zn} \\ \vdots \\ \boldsymbol{T}^{N_S}_{zn} \end{Bmatrix} = \begin{Bmatrix} \boldsymbol{u}^1_{zn} \\ \boldsymbol{u}^2_{zn} \\ \vdots \\ \boldsymbol{u}^{N_S}_{zn} \end{Bmatrix}. \tag{7}$$

The Lagrangian function Π of the system of N_S flexible strip foundations resting on a multilayered poroelastic half-plane as shown in Figure 1 can be expressed as

$$\Pi = \sum_{i=1}^{N_S} \left\{ V^i - U^i - \int_{-1}^{1} \left[\tfrac{1}{2} \left\{ T^i_z(\eta) + \alpha T^i_p(\eta) \right\} - f^i(\eta) \right] w^i_{st}(\eta)\, d\eta \right\}, \tag{8}$$

where V^i and U^i denote the kinetic and strain energies of the i-th strip foundation respectively and

$$V^i = \dot{\boldsymbol{\alpha}}^i \boldsymbol{M}^i_{st} (\dot{\boldsymbol{\alpha}}^i)^T, \qquad U^i = \boldsymbol{\alpha}^i \boldsymbol{H}^i_{st} (\boldsymbol{\alpha}^i)^T, \qquad i = 1, 2, 3, \ldots, N_S,$$

in which $\boldsymbol{\alpha}^i$ is a row vector whose elements are the generalized coordinates of the i-th foundation, that is, $\boldsymbol{\alpha}^i = \begin{bmatrix} \alpha^i_0 & \alpha^i_1 & \alpha^i_2 & \cdots & \alpha^i_{N_T} \end{bmatrix}$. The elements M^i_{mn} and H^i_{mn} of the matrices $\boldsymbol{M}^i_{st}$ and $\boldsymbol{H}^i_{st}$ are given by

$$M^i_{mn} = \frac{\rho^i_{st} h^i_{st} (a^i)^{m+n-1}}{2(m+n-1)} \left[1 - (-1)^{m+n-1}\right],$$

$$H^i_{mn} = \frac{E^i (h^i_{st})^2 (a^i)^{m+n-5}}{24\left[1 - (\nu^i_{st})^2\right]} \frac{(m-1)(m-2)(n-1)(n-2)}{(m+n-5)} \left[1 - (-1)^{m+n-5}\right],$$

where ρ^i_{st} is the density of the i-th foundation. In addition, $f^i(\eta)$ denotes the external loading acting on the i-th foundation and can be written as

$$f^i(\eta) = \sum_{m=0}^{N_L} \varphi^i_m \eta^m,$$

where φ^i_m is the coefficient of the loading function.

The Lagrange's equations of motion for the interaction problem shown in Figure 1 are given by

$$\frac{d}{dt}\left(\frac{\partial \Pi}{\partial \dot{\boldsymbol{A}}}\right) - \frac{\partial \Pi}{\partial \boldsymbol{A}} = 0, \tag{9}$$

where $\boldsymbol{A} = \begin{bmatrix} \boldsymbol{\alpha}^1 & \boldsymbol{\alpha}^2 & \boldsymbol{\alpha}^3 & \cdots & \boldsymbol{\alpha}^{N_S} \end{bmatrix}^T$. Substitution of (8) in (9) results in the following equations of motion to determine $\boldsymbol{\alpha}^i$ $(i = 1, 2, 3, \ldots, N_S)$:

$$\boldsymbol{Q}\boldsymbol{A} = \boldsymbol{B}, \tag{10}$$

where

$$\boldsymbol{Q} = -\omega^2 (\boldsymbol{M}_{st} + \boldsymbol{M}^T_{st}) + \boldsymbol{H}_{st} + \boldsymbol{H}^T_{st} + \boldsymbol{S} + \boldsymbol{S}^T,$$

and

$$\boldsymbol{M}_{st} = \operatorname{diag}[\boldsymbol{M}^i_{st}], \qquad \boldsymbol{H}_{st} = \operatorname{diag}[\boldsymbol{H}^i_{st}], \qquad \boldsymbol{S} = \operatorname{diag}[\boldsymbol{S}^i], \qquad \boldsymbol{B} = \begin{bmatrix} \boldsymbol{B}^1 & \boldsymbol{B}^2 & \boldsymbol{B}^3 & \cdots & \boldsymbol{B}^{N_S} \end{bmatrix}^T.$$

The elements of S^i_{mn} and B^i_m of the matrices $\boldsymbol{S}^i$ and $\boldsymbol{B}^i$ $(i = 1, 2, \ldots, N_S; m, n = 1, 2, \ldots, N_T + 1)$ are given by

$$S^i_{mn} = \frac{1}{2} \sum_{k=1}^{N_E} \Delta^i_k (\eta_k)^{m-1} \left(T^i_{z(n-1)k} + \alpha T^i_{p(n-1)k}\right), \qquad B^i_m = \sum_{k=1}^{N_L} \frac{\varphi^i_k (a^i)^{m+k-1}}{(m+k-1)} \left[1 - (-1)^{m+k-1}\right],$$

where Δ^i_k denotes the width of the k-th strip element of the i-th foundation.

The solution of a linear simultaneous equation system given by (10) yields the numerical values of the generalized coordinates α^i_n $(n = 0, 1, 2, \ldots, N_T; i = 1, 2, 3, \ldots, N_S)$ for a given foundation-half-plane system. Finally, vertical displacements, contact traction, and pore pressure jump can then be obtained by back substituting the generalized coordinates in (4) and (6) respectively.

4. Numerical results and discussion

Numerical results for dynamic interaction between a system of strip foundations subjected to vertical loading resting on a multilayered poroelastic half-plane are presented in this section. For impermeable strip foundations, the first step is to solve the system of linear simultaneous equations given by (5) to obtain the unknown contact traction T^i_{znk} and pore pressure jump T^i_{pnk} at each strip element of the i-th foundation ($i = 1, 2, 3, \ldots, N_S$) for each n value. For fully permeable foundations, (7) is solved for the unknown T^i_{znk}. This involves the computation of the influence functions $G^{ij}_{qr,kl}$ by solving (3). Since (3) is established in the Fourier transform space, it has to be solved for discrete values of ξ. The required influence functions are then determined by numerically integrating the inverse Fourier transform given by (2).

To perform the numerical integration, it is important to examine the singularities of the integrands. The main singularities are the branch points and poles that are complex-valued quantities with negative imaginary parts for all poroelastic materials due to the presence of some internal friction ($b \neq 0$). Therefore, the real ξ-axis is free from any singularities and the influence functions can be evaluated by direct numerical integration along the real ξ-axis when $b \neq 0$. For poroelastic materials with $b = 0$ and ideal elastic materials, 1% attenuation is used to ensure that the real ξ-axis is free from any singularity. In the present study, the numerical evaluation of the influence functions is performed by employing a globally adaptive numerical quadrature scheme [Piessens et al. 1983]. This scheme subdivides the interval of integrand and uses a 21-point Gauss–Kronrod rule to estimate the integral over each interval.

Convergence and numerical stability of the solution scheme were investigated with respect to the number of terms, N_T, in (4), and the number of strip elements, N_E, used to discretize the contact surface between the strip foundation and the half-plane. It was found that converged numerical solutions are obtained when $N_T \geq 8$ and $N_E \geq 20$.

The accuracy of the present solution scheme is verified by comparing with the existing solutions. The left side of Figure 3 shows a comparison of vertical compliance, $C_V = w_{st}(0)\mu^{(1)}/af_0$, of a rigid strip of width $2a$ subjected to a uniform load f_0 resting on a layered elastic half plane consisting of one homogeneous layer with a thickness of $2a$ and an underlying half-plane. Numerical solutions from the present scheme are compared with those presented by Israil and Ahmad [1989] for different values of $\mu^{(1)}/\mu^{(2)}$. The nondimensional frequency $\delta = \omega a\sqrt{\rho^{(1)}/\mu^{(1)}}$ is used in the comparison in this figure and all numerical results presented in this paper. It can be seen from the left side of Figure 3 that the two solutions agree very closely for all values of $\mu^{(1)}/\mu^{(2)}$.

The right side of Figure 3 presents a comparison of vertical impedance $K_V = F_0/\mu a w_{st}(0)$ of a permeable rigid strip of width $2a$ on a homogenous poroelastic half-plane subjected to a time-harmonic vertical force F_0. It is evident from the right side of Figure 3 that the solutions from the present scheme are in very good agreement with those given by Kassir and Xu [1988]. Note that the half-plane in the present study consists of 10 layers of equal thickness $0.2a$ and an underlying half-plane. A comparison of vertical impedance $K_V = f_0 a/\mu w_{st}(0)$ of a flexible strip on a homogenous elastic half-plane subjected to a uniform load of intensity f_0 is shown in Figure 4. The nondimensional relative rigidity, $\gamma = E_{st}h^3_{st}/12(1-\nu^2_{st})a^3\mu^{(1)}$, is used in the comparison. Excellent agreement is noted between the present solution and the solution given by Wang et al. [1991]. The accuracy of the present solution scheme is therefore verified by these independent comparisons.

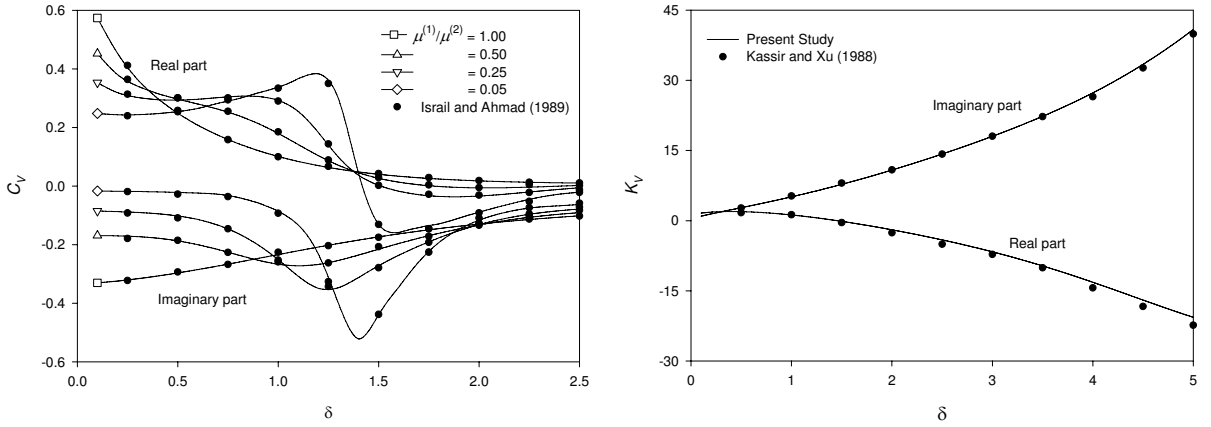

Figure 3. Comparison of (left) compliance of a rigid strip on a layered elastic half-plane, and (right) vertical impedance of a rigid strip on a homogenous poroelastic half-plane.

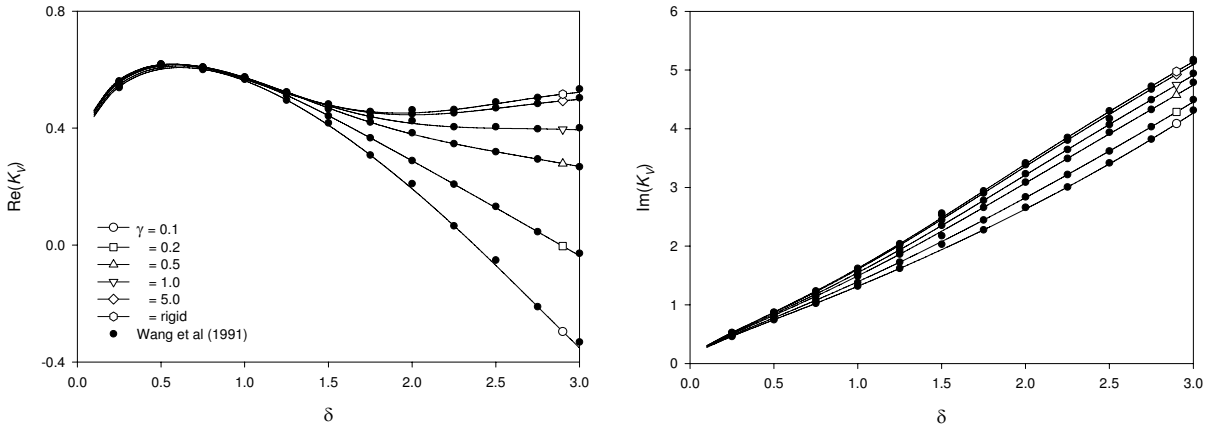

Figure 4. Comparison of vertical impedance of a flexible strip on an elastic half-plane.

Next, vertical vibrations of strip foundations resting on a multilayered poroelastic half-plane as shown in Figure 5 are studied. The strip foundations under consideration are either fully permeable or impermeable. The half-plane consists of two poroelastic layers bonded to an underlying poroelastic half-plane. The material properties of both layers and the underlying half-plane are given in Table 1. The first set of solutions corresponds to vertical vibrations of a single strip foundation on a multilayered poroelastic half-plane subjected to a uniform load of intensity f_0 as shown on the left side of Figure 5. Nondimensional vertical displacement at the center of the strip foundation, $w^*_{st}(0) = w_{st}(0)\mu^{(1)}/f_0 a$, is presented in Figure 6. Both fully permeable and impermeable foundations with different relative rigidity ratio $\gamma = 0.2, 0.5, 1.0, 5.0,$ and 100 are considered to investigate the influence of strip foundation rigidity and hydraulic boundary conditions at the contact surface. Numerical results presented in Figure 6 indicate that the variation of $w^*_{st}(0)$ with frequency is quite similar for fully permeable and impermeable strips although both real and imaginary parts of $w^*_{st}(0)$ are larger for the impermeable strip. Both real and imaginary parts of $w^*_{st}(0)$ decrease with increasing relative rigidity γ. The real part of $w^*_{st}(0)$ shows a

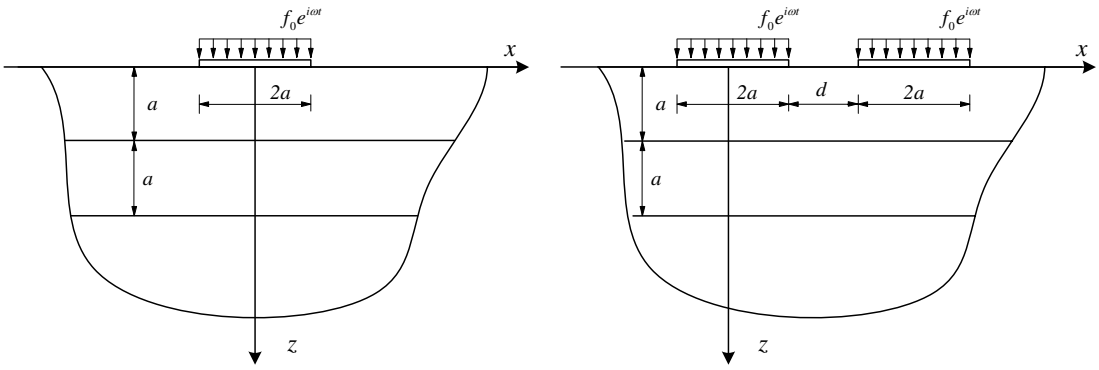

Figure 5. Flexible strip foundation systems considered in numerical study: (left) single strip and (right) two strips.

	μ	λ	M	ρ	ρ_f	$m^\dagger$	α	b
First layer	2.5	5.0	25.0	2.0	1.0	3.0	0.95	1.50
Second layer	1.25	1.88	18.8	1.6	1.0	1.8	0.98	0.75
Underlying half-plane	10.0	10.0	20.0	2.4	1.0	4.8	0.90	4.50

Table 1. Material properties of the layered systems considered in numerical study. Units: μ, λ and M in 10^8 N/m^2; ρ, ρ_f and m in 10^3 kg/m^3; b in 10^6 Ns/m^4.

change in sign within the frequency range $1.0 < \delta < 1.5$. The imaginary part of $w^*_{st}(0)$ remains negative throughout the frequency range $0 < \delta < 3.0$ and it is maximum when the corresponding real part of the solution is equal to zero. In addition, the strip foundation becomes virtually rigid when $\gamma \geq 100$.

Comparison of nondimensional central bending moment $M^*_{st}(0) = M_{st}(0)/f_0a^3$ shown in Figure 7 indicates that the bending moment of a strip foundation depends significantly on the relative rigidity γ and the hydraulic boundary condition at the contact surface. The bending moment at the center of the strip varies smoothly with frequency and the maximum values of real and imaginary parts of $M^*_{st}(0)$ are found when $1.0 < \delta < 1.5$. As expected, the magnitudes of both real and imaginary parts of $M^*_{st}(0)$ increase with increasing γ, and the bending moment at the center of an impermeable foundation is higher than that of the permeable one.

Figure 8 presents profiles of nondimensional displacement w^*_{st} of an impermeable strip foundation on the multilayered half-plane for $\gamma = 0.2, 0.5, 1.0, 5.0$, and 100, and $\delta = 0.5$ and 2.0. It can be seen from the left side of Figure 8 that both real and imaginary parts of displacement profiles depend significantly on relative rigidity and frequency. Both $\mathrm{Re}[w^*_{st}]$ and $\mathrm{Im}[w^*_{st}]$ are maximal at the center of the strip before monotonically decreasing at the strip edge. In addition, the displacements decrease with decreasing the relative rigidity γ, and the effect of γ is negligible when $\gamma > 100$.

Profiles of nondimensional contact traction $T^*_z = T_z/f_0$ and pore pressure jump $T^*_p = T_p/f_0$ under an impermeable strip foundation on the multilayered half-plane are presented in Figure 9 to investigate the load transfer mechanism between the strip and the half-plane. It is found that the contact traction under a flexible strip is distributed more uniformly than that under a rigid strip. Numerical results for

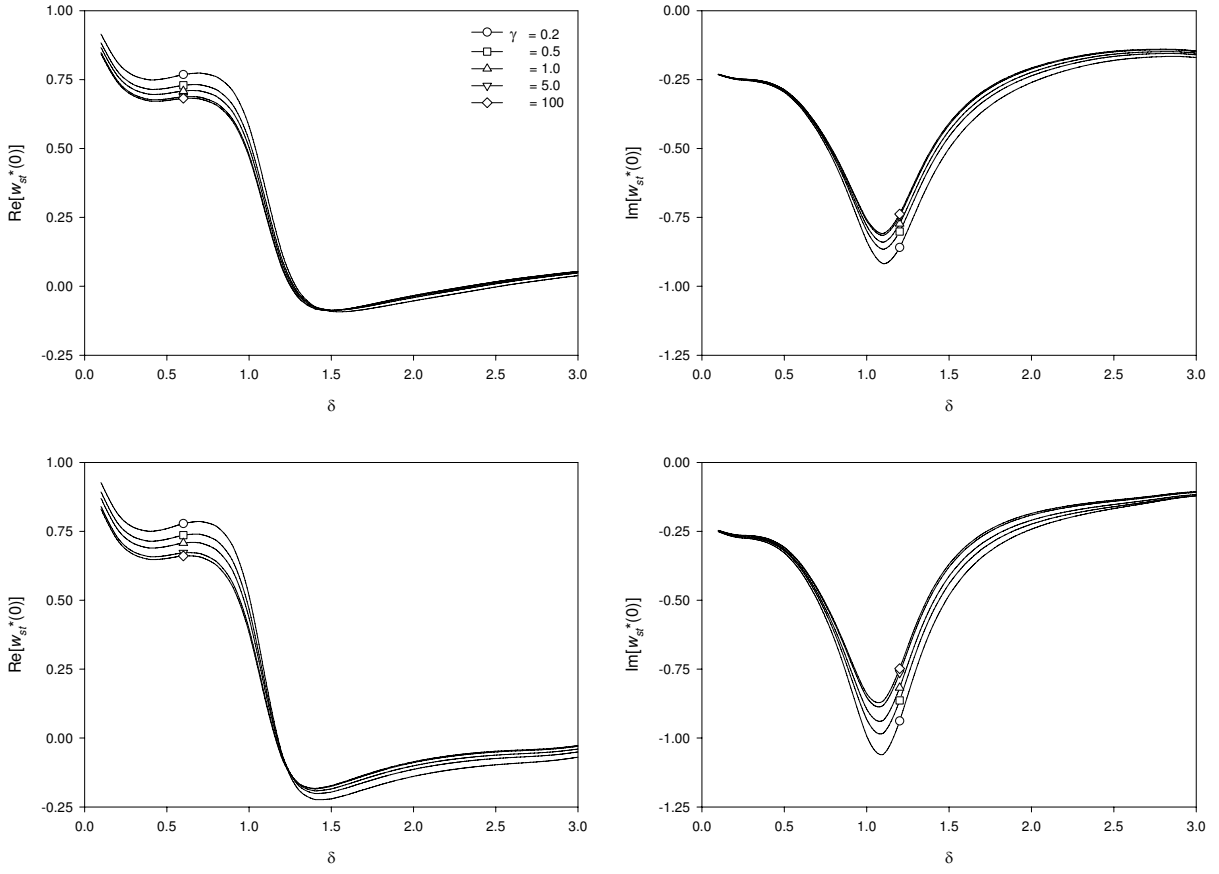

Figure 6. Displacement at the center of a flexible strip on a multilayered poroelastic half-plane: (top row) permeable strip and (bottom row) impermeable strip.

the contact traction presented in Figure 9 confirm the presence of classical singular behavior in both real and imaginary parts of T_z^* near the edge of the strip. Similar behavior was also observed for a rigid strip [Hryniewicz 1981] and a flexible strip [Wang et al. 1991] on a homogeneous elastic half plane. A comprehensive review on investigations of the exact local behavior of the contact traction in the vicinity of the foundation edge was given by Selvadurai [1979]. On the contrary, the pore pressure jump presented in Figure 9 is not singular near the strip edge. Its real and imaginary parts approach zero near the edge of both rigid and flexible strips. It is also found that larger pore pressure jump occurs at a higher frequency ($\delta = 2.0$) than at low frequency ($\delta = 0.5$). This implies that the load is carried by both solid and fluid phases at higher frequency, whereas at low frequency, the load transfer takes place through the solid skeleton. Similar behavior was also observed for the load transfer mechanism of a circular plate in a poroelastic medium [Zeng and Rajapakse 1999; Senjuntichai and Sapsathiarn 2003].

Figure 10 shows nondimensional central displacement $w_{st}^*(0)$ of an impermeable flexible strip foundation ($\gamma = 1.0$) on different poroelastic systems. Four poroelastic systems, namely a homogenous half plane, a homogenous layer of thickness a with an impermeable rigid base, and multilayered systems A

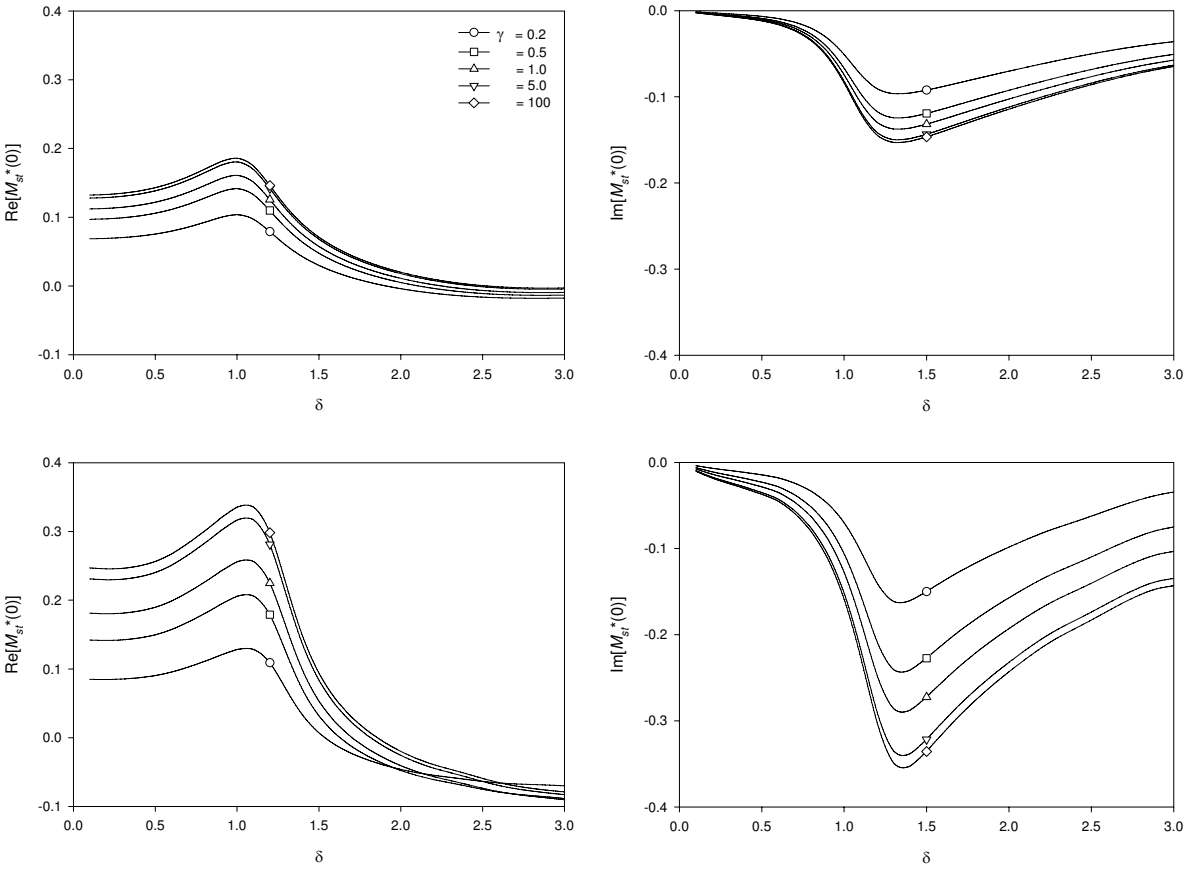

Figure 7. Bending moment at the center of a flexible strip on a multilayered poroelastic half-plane: (top row) permeable strip and (bottom row) impermeable strip.

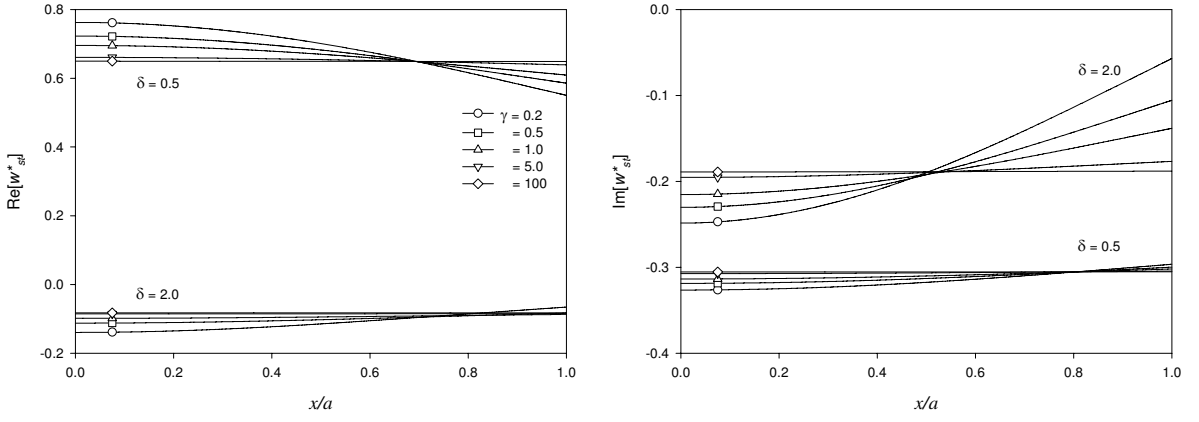

Figure 8. Displacement profiles of an impermeable strip on a multilayered poroelastic half-plane.

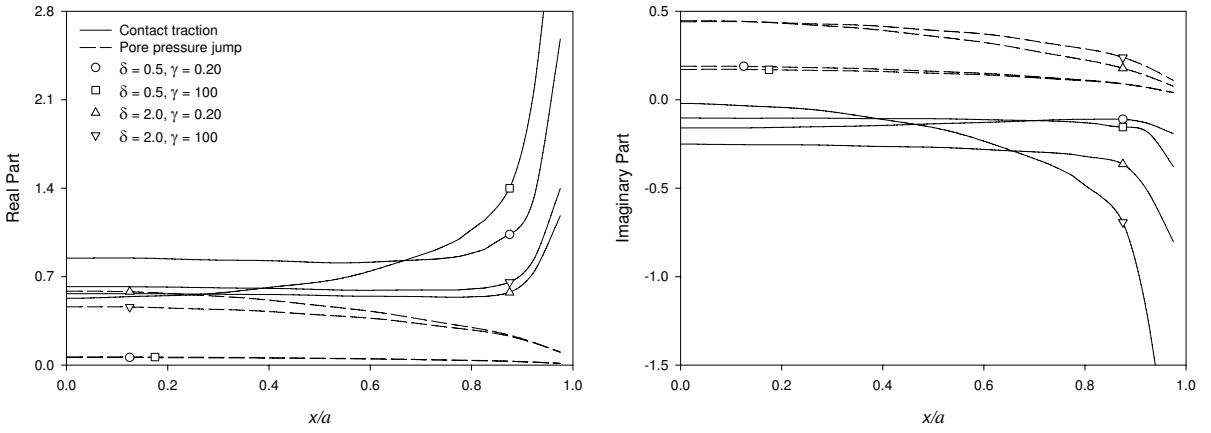

Figure 9. Profiles of contact traction and pore pressure jump under an impermeable strip on a multilayered poroelastic half-plane.

and B, are considered in this figure to investigate the influence of layering and poroelastic material parameters. The material properties of the homogeneous half-plane and the homogenous layer are identical to those of the first layer defined in Table 1. The geometries of the multilayered systems A and B are identical to those shown in Figure 5. The material properties of both systems are given in Table 1 except the internal friction between solid and fluid is neglected for both layers and the half-plane of system B ($b = 0$). The comparison of $w^*_{st}(0)$ presented in Figure 10 indicates substantial differences among three poroelastic systems. Both real and imaginary parts of $w^*_{st}(0)$ for the strip on the homogenous half-plane vary smoothly with δ whereas the strip displacement on the homogeneous layer shows oscillatory variation over the frequency range due to the standing wave generated between the surface and the rigid base. The difference in strip displacements corresponding to the multilayered systems A and B is mainly due to the parameter b. Note that all layers in system B have zero internal friction ($b = 0$) whereas system A consists of materials with nonzero b values. It is found that both real and imaginary parts of $w^*_{st}(0)$ in system A are smaller due to the presence of the internal friction between solid and fluid phases that makes this layered system more stiff and damped.

Numerical results corresponding to vertical vibrations of two impermeable strip foundations of width $2a$ subjected to uniform loading resting on a multilayered poroelastic half-plane as shown on the right side of Figure 5 with the properties given by Table 1 are presented next. The two strip foundations are identical and the distance between them is denoted by d. Variations of nondimensional displacement and nondimensional bending moment at the center of the left foundation with respect to nondimensional frequency are presented in Figures 11 and 12 respectively. Two values of the normalized distance between the two foundations $d/a = 1$ and 5 and the relative rigidity $\gamma = 0.2$, 0.5, 1.0, 5.0, and 100 are considered in these two figures. It should be noted that the influence of the normalized distance d/a was investigated by preparing plots similar to those shown in Figures 11 and 12 for different values of d/a. It was found that the effect of d/a on displacement and bending moment becomes negligible when $d/a > 15$.

Numerical results presented in Figures 11 and 12 indicate that the presence of the adjacent foundation significantly influences both displacement and bending moment. Both real and imaginary parts of $w^*_{st}(0)$ for the two-foundation systems ($d/a = 1.0$ and 5.0) presented in Figure 11 show more oscillatory variation

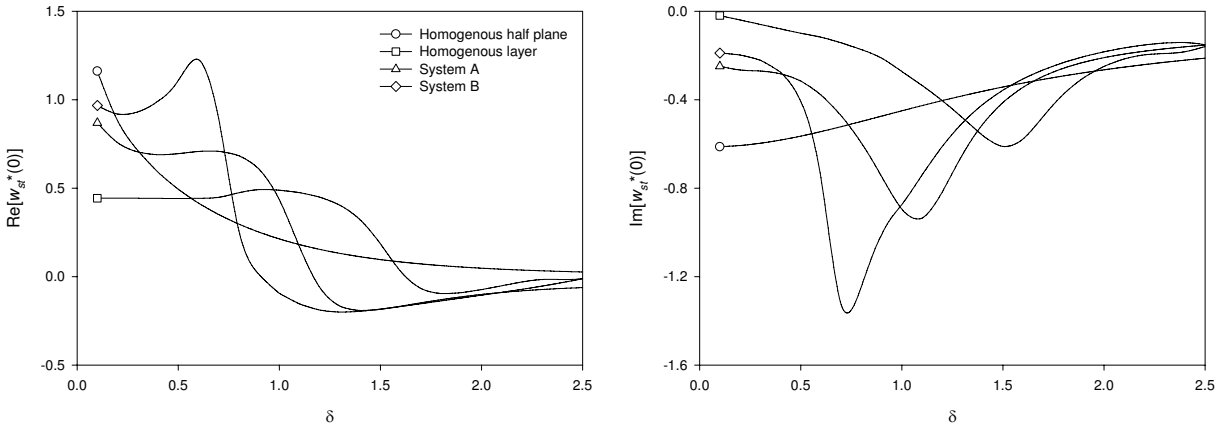

Figure 10. Displacement at the center of an impermeable strip ($\gamma = 1.0$) on different poroelastic systems.

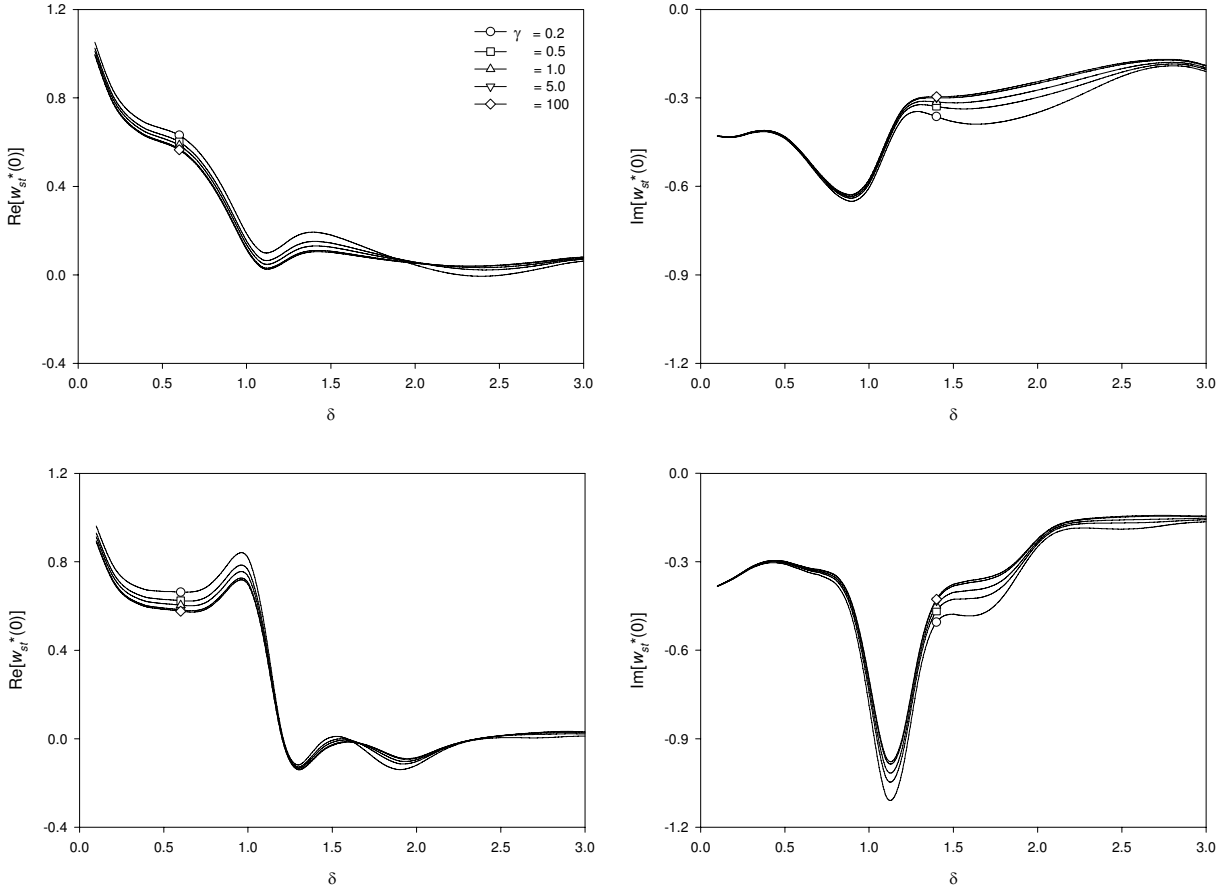

Figure 11. Displacement at the center of the left strip of two impermeable strip systems (see Figure 5, right side): (top row) $d/a = 1.0$ and (bottom row) $d/a = 5.0$.

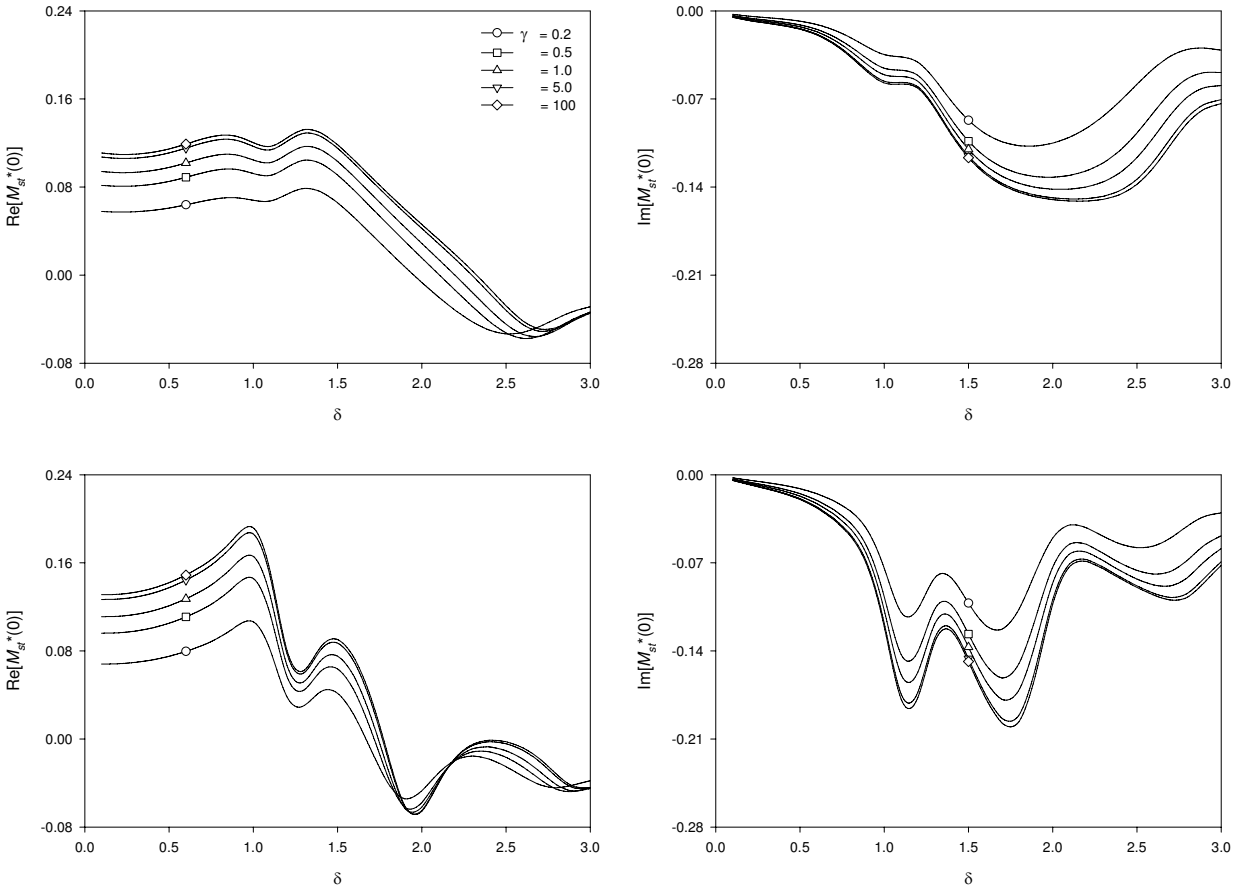

Figure 12. Bending moment at the center of the left strip of two impermeable strip systems (see Figure 5, right side) : (top row) $d/a = 1.0$ and (bottom row) $d/a = 5.0$.

with frequency when compared to smooth variations observed for a single strip foundation presented in Figure 6. The comparison of nondimensional displacement in Figure 11 for both two-foundation systems indicates differences in both magnitude and shape of $w^*_{st}(0)$. The real part of $w^*_{st}(0)$ for $d/a = 5.0$ shows a change sign near $\delta = 1.2$ whereas $\mathrm{Re}[w^*_{st}(0)]$ for the two-foundation system with $d/a = 1.0$ remains positive throughout the frequency range $0 < \delta < 3.0$. The imaginary part of $w^*_{st}(0)$ remains negative for $0 < \delta < 3.0$ and the maximum values are found near $\delta = 1.0$ for both $d/a = 1.0$ and 5.0. In addition, both real and imaginary parts of $w^*_{st}(0)$ decrease with increasing γ and the foundations become virtually rigid when $\gamma \geq 100$ similar to what observed for a single strip foundation in Figure 6.

The nondimensional bending moment shown for the two-foundation systems in Figure 12 indicates that both $\mathrm{Re}[M^*_{st}(0)]$ and $\mathrm{Im}[M^*_{st}(0)]$ exhibit more oscillatory variation with frequency than those observed for a single strip foundation in Figure 7. An important feature of the bending moment results revealed from Figure 12 is the notable dependence of both $\mathrm{Re}[M^*_{st}(0)]$ and $\mathrm{Im}[M^*_{st}(0)]$ on the distance d/a. The variation of both $\mathrm{Re}[M^*_{st}(0)]$ and $\mathrm{Im}[M^*_{st}(0)]$ with δ for the two-foundation system with $d/a = 5.0$ shows considerable oscillations, and it is quite different from that of a two-foundation system

with $d/a = 1.0$. Numerical results presented in Figure 12 also indicates that the relative rigidity γ has more significant influence on the bending moment than on the displacement, similar to what is observed in Figures 6 and 7 for a single strip foundation. Both real and imaginary parts of $M^*_{st}(0)$ for the two-foundation systems increase with increasing the relative rigidity γ and their magnitudes are lower than the corresponding solutions presented in Figure 7.

5. Conclusion

The dynamic interaction between a flexible strip foundation system under time-harmonic vertical loading resting on a multilayered poroelastic half plane is presented in this paper by using the coupled variational Green's function scheme together with a discretization technique. Both fully permeable and impermeable conditions at the contact surface between the foundations and the multilayered half-plane are considered. The required influence functions, which are computed by using the exact stiffness matrix method, correspond to a vertical strip load and fluid source applied at the surface of a multilayered poroelastic half-plane. The present numerical solutions are computationally stable and are in very good agreement with the existing solutions for both rigid and flexible foundations. Numerical results indicate that the dynamic response of the strip foundations depends significantly on the frequency of excitation, hydraulic boundary conditions, relative rigidity γ, poroelastic material properties and the distance between adjacent foundations. Both permeable and impermeable strip foundations show similar variations of displacement and bending moment with frequency, and higher magnitudes are observed in the impermeable one. With increasing the relative rigidity γ, the displacements of both single and multiple strip foundations decrease whereas their bending moments increase. The effect of the relative rigidity is negligible when $\gamma > 100$. In addition, the displacement and bending moment of the two-foundation system show significant dependence on both the distance between adjacent foundations and the frequency. It is also found that variations of displacement and bending moment with frequency show more considerable oscillations when $\delta > 1.5$.

References

[Biot 1941] M. A. Biot, "General theory of three-dimensional consolidation", *J. Appl. Phys.* **12**:2 (1941), 155–164.

[Biot 1956] M. A. Biot, "Theory of propagation of elastic waves in a fluid-saturated porous solid, I: Low-frequency range", *J. Acoust. Soc. Am.* **28**:2 (1956), 168–178. MR 24 #B110a

[Biot 1962] M. A. Biot, "Mechanics of deformation and acoustic propagation in porous media", *J. Appl. Phys.* **33**:4 (1962), 1482–1498. MR 27 #2218

[Bougacha et al. 1993] S. Bougacha, J. M. Roesset, and J. L. Tassoulas, "Dynamic stiffness of foundations on fluid-filled poroelastic stratum", *J. Eng. Mech.* (*ASCE*) **119**:8 (1993), 1649–1662.

[Chang-Liang 1974] V. Chang-Liang, *Dynamic response of structures in layered soils*, Ph.D. Thesis, MIT, Cambridge, MA, 1974, Available at http://nisee.berkeley.edu/elibrary/Text/200612062.

[Gazetas and Roesset 1976] G. Gazetas and J. M. Roesset, "Forced vibrations of strip footings on layered soils", pp. 115–131 in *Methods of structural analysis: Proceedings of the National Structural Engineering Conference* (Madison, WI, 1976), edited by W. E. Saul and A. H. Peyrol, ASCE, New York, 1976.

[Hryniewicz 1981] Z. Hryniewicz, "Dynamic response of a rigid strip on elastic half-space", *Comput. Methods Appl. Mech. Eng.* **25**:3 (1981), 355–364.

[Israil and Ahmad 1989] A. S. M. Israil and S. Ahmad, "Dynamic vertical compliance of strip foundations in layered soils", *Earthquake Eng. Struct. Dyn.* **18**:7 (1989), 933–950.

[Japón et al. 1997] B. R. Japón, R. Gallego, and J. Domínguez, "Dynamic stiffness of foundations on saturated poroelastic soils", *J. Eng. Mech.* (*ASCE*) **123**:11 (1997), 1121–1129.

[Karasudhi et al. 1968] P. Karasudhi, L. M. Keep, and S. L. Lee, "Vibratory motion of a body on an elastic half plane", *J. Appl. Mech.* (*ASME*) **35** (1968), 697–705.

[Kassir and Xu 1988] M. K. Kassir and J. Xu, "Interaction functions of a rigid strip bonded to saturated elastic half-space", *Int. J. Solids Struct.* **24**:9 (1988), 915–936.

[Kokkinos and Spyrakos 1991] F. T. Kokkinos and C. C. Spyrakos, "Dynamic analysis of flexible strip-foundations in the frequency domain", *Comput. Struct.* **39**:5 (1991), 473–482.

[Luco and Westmann 1972] J. E. Luco and R. A. Westmann, "Dynamic response of rigid footing bonded to an elastic half space", *J. Appl. Mech.* (*ASME*) **39** (1972), 527–534.

[Piessens et al. 1983] R. Piessens, E. de Doncker-Kapenga, C. W. Überhuber, and Kahaner, *QUADPACK: A subroutine package for automatic integration*, Springer Series in Computational Mathematics **1**, Springer, Berlin, 1983. MR 85b:65022

[Rajapakse and Senjuntichai 1995] R. K. N. D. Rajapakse and T. Senjuntichai, "Dynamic response of a multi-layered poroelastic medium", *Earthquake Eng. Struct. Dyn.* **24**:5 (1995), 703–722.

[Selvadurai 1979] A. P. S. Selvadurai, *Elastic analysis of soil-foundation interaction*, Elsevier, Amsterdam, 1979.

[Senjuntichai and Rajapakse 1994] T. Senjuntichai and R. K. N. D. Rajapakse, "Dynamic Green's functions of homogeneous poroelastic half-plane", *J. Eng. Mech.* (*ASCE*) **120**:11 (1994), 2381–2404.

[Senjuntichai and Rajapakse 1996] T. Senjuntichai and R. K. N. D. Rajapakse, "Dynamics of a rigid strip bonded to a multilayered poroelastic medium", pp. 353–370 in *Mechanics of poroelastic media*, edited by A. P. S. Selvadurai, Solid Mechanics and its Applications **41**, Kluwer, Dordrecht, 1996.

[Senjuntichai and Sapsathiarn 2003] T. Senjuntichai and Y. Sapsathiarn, "Forced vertical vibration of circular plate in multilayered poroelastic medium", *J. Eng. Mech.* (*ASCE*) **129**:11 (2003), 1330–1341.

[Sneddon 1951] I. Sneddon, *Fourier transform*, McGraw-Hill, New York, 1951.

[Spyrakos and Beskos 1986] C. C. Spyrakos and D. E. Beskos, "Dynamic response of flexible strip-foundations by boundary and finite elements", *Soil Dyn. Earthq. Eng.* **5**:2 (1986), 84–96.

[Spyrakos and Xu 2004] C. C. Spyrakos and C. Xu, "Dynamic analysis of flexible massive strip-foundations embedded in layered soils by hybrid BEM–FEM", *Comput. Struct.* **82**:29–30 (2004), 2541–2550.

[Wang et al. 1991] Y. Wang, R. K. N. D. Rajapakse, and A. H. Shah, "Dynamic interaction between flexible strip foundations", *Earthquake Eng. Struct. Dyn.* **20**:5 (1991), 441–454.

[Warburton et al. 1971] G. B. Warburton, J. D. Richardson, and J. J. Webster, "Forced vibrations of two masses on an elastic half space", *J. Appl. Mech.* (*ASME*) **38** (1971), 148–156.

[Wong and Luco 1986] H. L. Wong and J. E. Luco, "Dynamic interaction between rigid foundations in a layered half-space", *Soil Dyn. Earthq. Eng.* **5**:3 (1986), 149–158.

[Zeng and Rajapakse 1999] X. Zeng and R. K. N. D. Rajapakse, "Vertical vibrations of a rigid disk embedded in a poroelastic medium", *Int. J. Numer. Anal. Methods Geomech.* **23**:15 (1999), 2075–2095.

Received 12 Jul 2007. Revised 29 Jun 2008. Accepted 22 Sep 2008.

TEERAPONG SENJUNTICHAI: fcetsj@eng.chula.ac.th
Department of Civil Engineering, Chulalongkorn University, Bangkok 10330, Thailand

WICHAIRAT KAEWJUEA: iwichairat@yahoo.com
Department of Civil Engineering, Chulalongkorn University, Bangkok 10330, Thailand